

Joint analysis of refractions with surface waves: An inverse solution to the refraction-traveltime problem

Julian Ivanov¹, Richard D. Miller¹, Jianghai Xia¹, Don Steeples², and Choon B. Park¹

ABSTRACT

We describe a possible solution to the inverse refraction-traveltime problem (IRTP) that reduces the range of possible solutions (nonuniqueness). This approach uses a reference model, derived from surface-wave shear-wave velocity estimates, as a constraint. The application of the joint analysis of refractions with surface waves (JARS) method provided a more realistic solution than the conventional refraction/tomography methods, which did not benefit from a reference model derived from real data. This confirmed our conclusion that the proposed method is an advancement in the IRTP analysis. The unique basic principles of the JARS method might be applicable to other inverse geophysical problems.

INTRODUCTION

Several factors contribute to the nonuniqueness issue of the inverse refraction-traveltime problem (IRTP) that are not sufficiently addressed by conventional and currently employed inversion algorithms (Ivanov et al., 2005b). As a result, solutions can include a wide range of possible earth models that adequately fit the observed first-arrival data.

Most inversion-based solutions of geophysical problems, including the IRTP, are nonunique because, by their nature, these problems consist of a finite number of measured data points that are used to define a continuously varying earth structure (Backus and Gilbert, 1967, 1968). Nonuniqueness also results from error in the data. This is especially true when the inverse problem is unstable, such as when small perturbations in the data (equivalent to the amount of data error) cause large changes in the solution. A significant amount of work has been done studying the effects of data errors on the solution and the resulting instability, as well as on the inexact-data nonuniqueness of linear problems (Backus and Gilbert, 1970; Meju, 1994).

Even for simple models and exact data, the IRTP has been found to have many possible solutions (Slichter, 1932; Healy, 1963; Ackerman et al., 1986; Burger, 1992; Lay and Wallace, 1995). Such exact-data nonuniqueness (EDNU) has been associated with a variable number of model parameters (i.e., 2-, 3-, and n-layer models could provide the same solution). The IRTP nonuniqueness has not been examined sufficiently for cases with a fixed number of model parameters, yet these are of particular interest when solving multiparameter inverse problems. Studies of this type are important because they provide insight about the topology (number of local and global minimums) of the minimized objective function (OF; i.e., the match between modeled and observed data) and the possible behavior of inversion algorithms (Ivanov et al., 2005a).

The IRTP is continuously nonunique even when one assumes that the data and the model are error free (Ivanov et al., 2005b). The authors closely examined the IRTP for a fixed number of parameters using a simple three-layer model and first-arrival data that had only two apparent slopes (apparent velocities Figure 1). Varying the parameters of the second layer produces a continuous range of possible solutions (Figure 2), even assuming infinite, error-free data. Existing refraction/tomography inversion algorithms do not address this type of continuous EDNU. Furthermore, providing a two-layer-model solution to observed first arrivals that have two apparent slopes is equivalent to choosing one point in the nonuniqueness valley (Ivanov et al., 2005b).

Continuous exact-data nonuniqueness

In general, nonuniqueness is resolved by using a priori information (API) (Zhdanov, 2002). API can be defined as information not contained in the original equation (Menke, 1989, p. 48), or, as all other information beyond what we have chosen to call data (Jaynes, 2003, p. 88). Therefore, choosing a two-layer-model is justified only if there is API supporting such a choice. Otherwise, the solution

Manuscript received by the Editor May 2, 2006; revised manuscript received May 2, 2006; published online November 3, 2006.

¹University of Kansas, Kansas Geological Survey, 1930 Constant Avenue, Lawrence, Kansas 66047. E-mail: jivanov@kgs.ku.edu; rmiller@kgs.ku.edu; jxia@kgs.ku.edu; park@kgs.ku.edu.

²University of Kansas, Department of Geology, 1475 Jayhawk Boulevard, Lawrence, Kansas 66045. E-mail: don@ku.edu.

© 2006 Society of Exploration Geophysicists. All rights reserved.

might be significantly different than the true solution, which could be positioned anywhere in the nonuniqueness valley (Figure 2) (Ivanov et al., 2005b).

The IRTP has a multidimensional hypervalley of nonuniqueness. Further EDNU analysis of the IRTP (Ivanov et al., 2005b) showed more hidden layers could be included, thereby increasing the number of model parameters while preserving the observed first-arrival data with only two apparent slopes. Following the same line of thought, it was reasoned that an N -parameter IRTP would have an $(N-a)$ -dimensional hypervalley of nonuniqueness (where a is a very small number of uniquely identifiable parameters, e.g., the velocities of the uppermost and the very bottom layer). Such multiparameter EDNU can be uniquely solved only by involving significant amounts of API.

The problem with current IRTP algorithms is that they do not target EDNU. Many of them address the nonuniqueness factors mentioned earlier by using stabilizing functionals (e.g., smoothing constraints; Zhdanov et al., 2002). However, The stabilizing functionals might bias the resulting IRTP solutions toward a specific location in the nonuniqueness valley without dependence on real world evidence (Ivanov et al., 2005b).

We propose to use shear-wave velocity (V_s) information (estimated using surface-wave dispersion-curve inversion) to create a reference compressional-wave velocity (V_p) model as a means of reducing the continuous range of possible solutions. Of course, the best

way to resolve the problem is to use ample accurate API from sample measurements of velocities (e.g., from wells), but such an approach is often impractical.

Results from the newly developed joint analysis of refractions with surface waves (JARS) method appear more realistic than solutions provided by some of the most popular IRTP algorithms, such as the Generalized Reciprocal Method (GRM) (Palmer, 1980) or traditional first- and second-degree smoothing regularization refraction-tomography algorithms. In addition, the JARS solution is better justified because it is based on an API model derived from another seismic method (and thus affected by some of the same physical properties) instead of being based on assumptions (e.g., smoothness of the earth model), which is the usual case with other algorithms.

JARS METHOD

Shear-wave velocity estimation

The first step in the proposed method is the acquisition of a V_s earth model from surface-wave analysis. The advances in surface-wave analysis that have come with the development of the multi-channel analysis of surface waves (MASW) method (Park et al., 1999a; Xia et al., 1999a) permit confident estimates of shear-wave velocities (V_s). The practical application of MASW has provided reliable correlations to drill data (Xia et al., 2000). Using MASW, Miller et al. (1999a) mapped bedrock horizons to within 0.3 m (1 ft) at depths of about 4.5–9 m (15–30 ft), confirming their results with numerous borings. The MASW method has been applied to problems such as the characterization of pavements (Park et al., 2001; Ryden et al., 2001), the study of Poisson's ratio (Ivanov et al., 2000a), the investigation of sea-bottom sediment stiffness (Park et al., 2000; Ivanov et al., 2000b), the detection of dissolution features (Miller et al., 1999b), and the measurement of S-wave velocity as a function of depth (Xia et al., 1999b). Because of its high reliability in practice, we prefer the MASW method to other methods for shear-wave velocity estimation [e.g., shear-wave refraction, spectral analysis of surface waves (SASW), etc.].

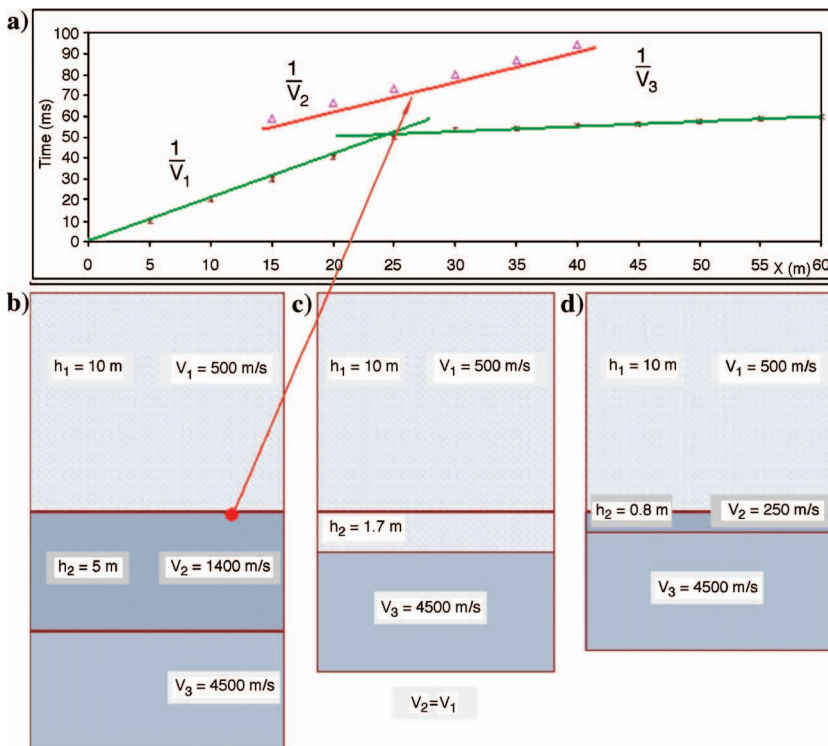


Figure 1. A simple, refraction nonuniqueness problem demonstrated using refraction traveltimes from a set of a source and receivers. (a) Three different three-layer models can generate the same first arrivals. Layers 1 and 3 have the same thickness and velocity parameters in each model, while the parameters vary for layer 2. (b) Layer 2 is a high-velocity layer. (c) Layer 2 has the same velocity as layer 1. (d) Layer 2 is a low-velocity layer. The figure is derived from Burger (1992). The second layer thickness is rounded for better display.

Approximation of a reference compressional-wave velocity model

The next step is the generation of a reference V_p model. Here, we propose to use V_s (estimated by using the MASW method) to estimate a reference V_p model. Such a model can be generated using any available information about the overall distribution of the V_p/V_s ratio at a specific site. When such API is not available, a more general assumption, namely that the general trend of V_p follows that of V_s , can be employed. We chose the latter case for testing our method because this situation seems to be most commonly encountered in practice.

The idea that the V_p trend is related to V_s is based on the observations of many researchers (Lay and Wallace, 1995) and on the fact that both parameters are related through elastic moduli.

Geologic layers go through various processes during and after deposition, including compaction, desiccation, cementation, crystallization, and metamorphism. These processes generally affect elastic moduli in a somewhat consistent fashion. Therefore, as the shear modulus increases with compaction, both V_p and V_s will increase. That is,

$$V_p = \sqrt{\frac{\lambda + 2\mu}{\rho}}, \quad (1)$$

$$V_s = \sqrt{\frac{\mu}{\rho}}, \quad (2)$$

where ρ is density of matter, μ is the shear modulus, and λ is Lamé's second constant.

We can generate a reference 2D V_p section using a 2D V_s section as the starting point. Once the V_s results are calculated, a rough V_p model that preserves the earth-model structures from V_s can be obtained initially by scaling the 2D V_s section to a constant. This pseudo V_p section is then used to estimate the first forward model and compare the calculated data with the observed results. These steps can be repeated by using an improved constant to achieve a better match between the calculated and the observed data. This type of iterative processing continues until the match between the calculated and observed data becomes acceptably close. This generally occurs when improving the match requires changing parts of the pseudo 2D V_p section. Further changes to the empirically derived constant consist of slight increases for the shallow section and slight decreases for the deeper parts, as necessary to accommodate depth-dependent V_p/V_s trends. In this fashion, the rough V_p earth model can be used as an initial model and reference API during the IRTP inversion.

Traditional inversion algorithm

To solve the highly nonlinear (Nolet, 1987) inverse refraction problem, we apply the Tichonov regularization (Tikhonov and Arsenin, 1977; Zhdanov, 2002) by adding the API to the system of first arrival traveltimes equations and seeking the least-squares solution of the system:

$$\begin{bmatrix} \mathbf{L} \\ \beta \mathbf{D}_d \\ \lambda \mathbf{D}_s \end{bmatrix} [\mathbf{s}^{est}] = \begin{bmatrix} \mathbf{t}^{obs} \\ \dots \\ \beta \mathbf{s}^a \\ \lambda \mathbf{h} \end{bmatrix}, \quad (3)$$

where matrix \mathbf{L} represents the ray lengths through the earth model, \mathbf{s}^{est} is the model vector of the estimated velocity field, and \mathbf{t}^{obs} is a vector of observed first-arrival times. The API is present in the form of weighted smoothing (λ : not to be confused with Lamé's constant or wavelength) and damping (β) constraints. Smoothing is applied as a remedy for indeterminacy and instability. Damping constrains the solution to the neighborhood of the reference a priori model \mathbf{s}^a . \mathbf{D}_d is the matrix containing weights for the reference model (usually set to a value of 1), \mathbf{D}_s is the matrix containing the smoothing constraints (first, second, or higher derivative), and \mathbf{h} is a vector usually set to 0, resulting in a maximum degree of smoothness.

Expanding the inversion scheme with an approximate reference model

The relationship shown as equation 3 can be expanded to accommodate this type of additional API, while still preserving the accurate a priori model-damping component as follows:

$$\begin{bmatrix} \mathbf{L} \\ \beta \mathbf{D}_d \\ \beta_2 \mathbf{D}_d \\ \lambda \mathbf{D}_s \end{bmatrix} [\mathbf{s}^{est}] = \begin{bmatrix} \mathbf{t}^{obs} \\ \beta \mathbf{s}^a \\ \beta_2 \mathbf{s}^{aa} \\ \lambda \mathbf{h} \end{bmatrix}, \quad (4)$$

where \mathbf{s}^{aa} is the approximate API representing the reference model and β_2 is the corresponding weighting coefficient.

Two damping coefficients are necessary for the two sets of damping constraints, each having a different weight. The different types of API need to be treated differently during refraction-tomography inversion, and the accurate component (usually very sparse) should receive greater weight than the approximate. The smaller the weight of the approximate API, the greater variance the solutions can have from the reference model.

Adjusting the direction of smoothing constraints

It is necessary for most geophysical problems, to apply smoothing during inversion to decrease the nonuniqueness that results from erroneous data and undetermined zones (Meju, 1994). However, smoothing can preferentially favor certain equally possible exact-data solutions (Ivanov et al., 2005b). To avoid this, our proposed method applies smoothing constraints in the horizontal direction only, generally consistent with the expected dominant layering of geologic units. As a result, the solution of the JARS method in the

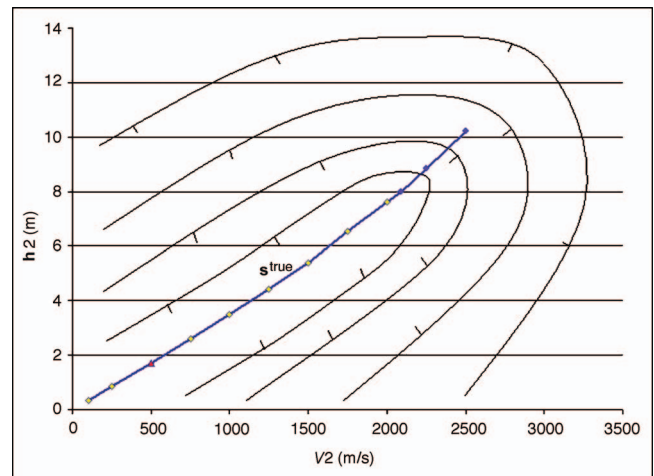


Figure 2. A 2D map of the mismatch error (objective) function E demonstrating hidden-layer nonuniqueness of the second layer shown in Figure 1 (thick line with diamonds). For any velocity, V_2 , an appropriate thickness can be found such that the first arrivals remain identical. Below 500 m/s is the region of the low-velocity hidden layer. Above 500 m/s is the region of the high-velocity hidden layer. At 500 m/s is the same-velocity hidden layer (triangle). At an upper-bound velocity of 2090 m/s, the refractions from the second layer start to appear as first arrivals but are still hardly distinguishable up to 2500 m/s (circles). Thin contour lines show a 2D map of the mismatch error-function E , and the direction of the ticks indicates lesser values. The true solution \mathbf{s}^{true} may be anywhere in the nonuniqueness valley.

vertical direction is influenced only by the reference V_p model derived from the V_s results. The solution in the horizontal direction is influenced by both the reference V_p model and the smoothing constraints. Smoothing is still preserved in the inversion scheme to account for the other sources of nonuniqueness, as described earlier.

Even though the derived reference V_p model is approximate, it helps the inversion algorithms define the entrance of the nonuniqueness valley and select a reasonable region in that same valley to locate the solution (Figure 3). Based on the general-trend assumption, supported by formulas 1 and 2, the true solution is expected somewhere near the reference model.

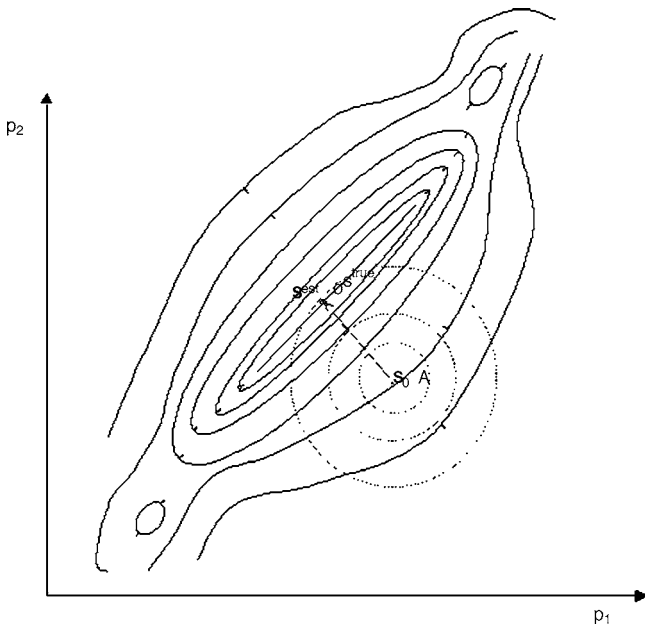


Figure 3. Two-dimensional continuous nonuniqueness. A 2D map of the mismatch error (objective) function E . Initial model s_0 strike used for approximate API. The obtained solution, s^{sol} , is at minimum distance from the reference (approximate API, s_0) and is within proximity of the true solution (s^{true}).

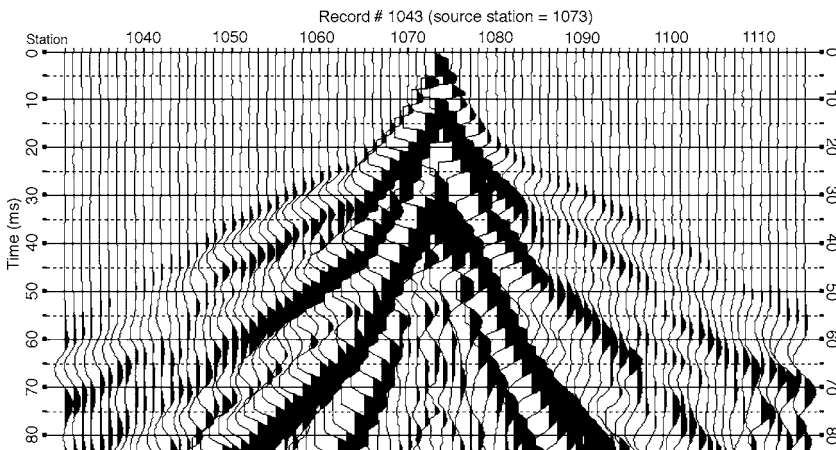


Figure 4. A shot gather from the seismic data set collected in the Sonora Desert, Arizona, USA.

DATA EXAMPLE

We applied the JARS method to seismic data collected in the Sonora Desert, Arizona, USA. The entire data set was recorded using a fixed spread of 240 receiver stations spaced at 1.2 m apart to record the seismic wavefield. Our source was a rubberband assisted weight drop (RAWD) (a mass of 50 kg accelerating through 0.5 m and impacting a striker plate of equal mass). It provided a repeatable broadband, high-energy, minimum-phase waveform. The seismic energy was recorded using a 240-channel Geometrics Strata View seismograph and single 10-Hz geophones. To maximize redundancy and economics, the source spacing was 4.8 m inline and 1.2 m off-line. Data from 13 shot stations, equally spread along the line, were selected to solve the IRTP (Figure 4). First arrivals are characterized by two apparent slopes, which were picked using the commercial software, Picker [part of the Green Mountain Geophysics (GMG) refraction package].

We obtained a 2D V_s image by applying the MASW method to the data from the 13 shot gathers along each profile using SurfSeis software (a proprietary software package of the Kansas Geological Survey). These 2D V_s data were rescaled (following the general-trend assumption) to create a corresponding V_p model for use as an initial model and as a reference API for the JARS method to find a possible solution to the IRTP (Figure 5a). For comparison, three other possible IRTP solutions were obtained without the benefit of the V_s information. One refraction-tomography solution (Figure 5b) was obtained by applying second-degree smoothing regularization (Delpat-Jannaud and Lailly, 1993), a method by Zhang and Toksöz (1998). Another tomography solution (Figure 5c) was calculated using first-degree smoothing regularization (the most common type) with FathTomo software (part of the GMG refraction package). The fourth solution (Figure 5d) was acquired using the GRM (Palmer, 1980), also part of the GMG refraction package. Using the GRM solution as an initial model, the two tomography solutions converged to a traveltimes misfit of 2 ms.

The JARS solution appears most geologically realistic based on the geologic model widely accepted at this site. Channel-like features in the top left portion of the image do not appear on either tomography-only or delay-time solutions. All the acquired solutions were visually examined and evaluated as to how well they matched our geologic expectations for the investigated site. This qualitative

approach is deemed acceptable because we consider all IRTP solutions equally plausible from a numerical perspective. They can be regarded as points along a multiparameter nonuniqueness valley, similar to the two-parameter three-layer model shown in Figure 2. The numerical nonuniqueness could only be resolved using extreme quantities (as indicated by EDNU studies) of sample velocity measurements, a characteristic that is very rare in reality.

The JARS-derived V_p/V_s -ratio map (Figure 6a) appears most realistic based on known geology. We produced corresponding 2D V_p/V_s -ratio maps using the MASW 2D V_s results (Figure 6a-d) and used them as an additional qualitative tool to assess the V_p solutions. Value trends derived using standard tomography and refraction solutions seem sporadic and unnatural (Figure 6b-d). Our visual estimate of quality was supported by the

calculated standard deviations for each of the V_p/V_s -ratio maps: 0.46, 0.59, 0.64, and 0.83 (Figures 6a-d). Standard deviation is a measure of variability (Menke, 1989), and therefore can be used as an indirect indicator of the likelihood of a calculated result. All these qualitative evaluations provide information about the likelihood of delay-time and tomography-only solutions. Solutions obtained without incorporating site specific calculations of V_s , although possible, were considered to be unlikely based on existing site specific information.

Selecting regularization parameters (weight coefficients β , β_2 , and λ) is considered subjective (Claerbout, 1992, p. 82), regardless of the algorithm used (Tichonov and Arsenin, 1977; Hansen, 1998; Xia et al., 2005). No matter what form it takes, API quantifies expectations about the solution that are not based on actual data (Menke, 1989, p. 48). For consistency with this particular data set, we chose to have the weight of the smoothing constrains for all tomography solutions be identical with that of the GMG solution. The weight of the reference pseudo V_p model (β_2) was selected to be three times smaller than the weight of the smoothing constraints. The qualitative selection of the final V_p solution was influenced by the overall smoothness of the corresponding V_p/V_s ratio map.

The JARS method was not improved relative to the other methods by the incorporation of a better initial model. To demonstrate this, the initial model utilized for formulating the JARS solution was used to calculate another GMG tomography-inversion solution. The new-

ly obtained GMG solution for the most part possessed less than a 3% deviation from the first GMG solution, which used refraction results as an initial model. Therefore it is not displayed on a separate figure. This comparison illustrates that most current refraction-tomography algorithms in common use are biased internally and do not depend heavily on the initial model. Instead, they rely most likely upon stabilizing functionals, such as smoothing constraints. Without involving any API, there is no way to determine if the solution obtained is true or even close to the true solution.

The JARS V_p/V_s ratio maps can provide a qualitative approximation of the true V_p/V_s ratio distribution (or its Poisson's ratio version). Such information is often sought for solving environmental and engineering problems, and in some cases, it can provide insights into material properties that improve lithological identification and geologic interpretation. These byproduct results should be used with caution because they are strongly influenced by the subjectively selected weighting coefficient of the reference model. A JARS V_p/V_s ratio map obtained using a reasonable smoothness weighting and a relatively low (but not zero) standard deviation can be used as a rough guide to the real V_p/V_s ratio distribution. However, the principal use of a JARS V_p/V_s ratio section should mainly be used as a qualitative evaluation of the JARS inversion results. Determining the true V_p/V_s ratios must be based on accurate data from site-specific measurements.

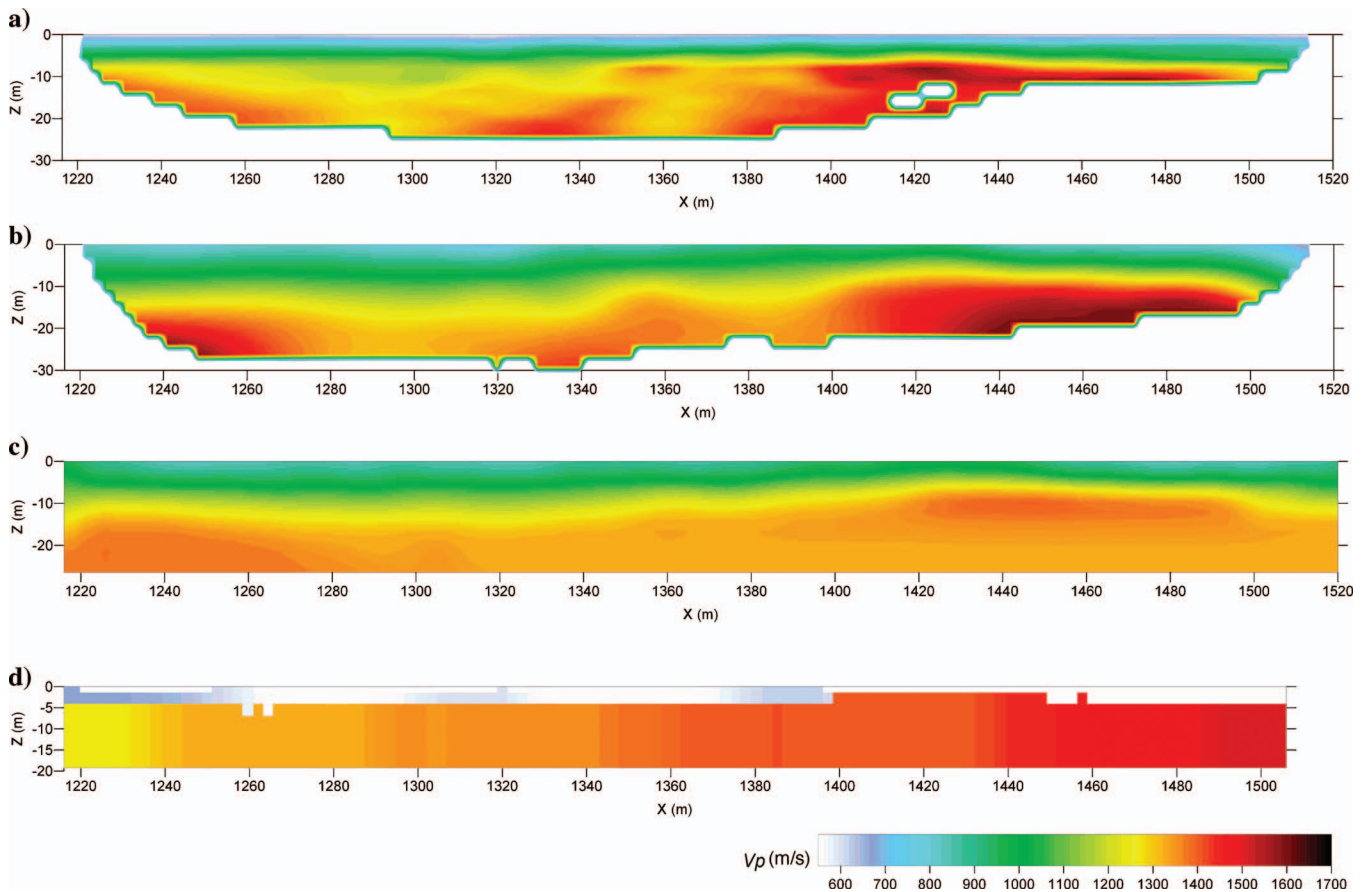


Figure 5. Inverse refraction traveltimes V_p solutions for the seismic data set collected in the Sonora Desert, Arizona, USA. (a) JARS method with second-order horizontal smoothing constraints; (b) Tomography only with second-order smoothing constraints; (c) Tomography only with first-order smoothing constraints; and (d) GRM two-layer solution (Kriging was applied to the solution data to create the image).

DISCUSSION

We have provided evidence to support the premise that the JARS reference V_p model provides better API than the existing stabilizing functionals — used by most algorithms for solving the IRTP — because it has both quantitative and qualitative properties. It is qualitative because it is approximate (includes a rough rescale of V_s and a subjectively selected weighting coefficient), and it is quantitative because it is based on real parameter estimates (V_s results). Stabilizing functionals in routine commercial use, on the other hand, provide purely qualitative API. Most often the type and extent of API is based on assumptions and not on real data from actual measurements (for example, from well logs). From a practical perspective, the approximate API derived from JARS is probabilistically a better option than assuming the degree of smoothing for the real geologic model (which may range from sharp maximum-gradient to gradual minimum-gradient models).

We used smoothing constraints in our inversion approach because they are the most popular regularization parameter for use in inversion algorithms (Constable et al., 1987; Meju, 1994). Their use also facilitated the comparison of our technique with other inversion algorithms. Researchers have implemented other stabilizing functions, such as total variation (TV) (Rudin et al., 1992), minimal support (MS; Last and Kubik, 1983), and minimal-gradient support (MGS), (Portniaguine and Zhdanov, 1999) for solving the inverse

problem. Just like the bias associated with independent use of smoothing constraints, using stabilizing functions alone would strongly influence the IRTP solution toward a certain location in the nonuniqueness valley.

The JARS system shown in equation 4 is less ill-conditioned than the traditional system shown in equation 3. It is common when solving tomography problems for the original matrix L to not have rank N (number of parameters). Usually, adding a stabilizing functional (e.g., smoothing constraints) helps minimize this problem. In addition, the inclusion of abundant API (from surface-wave analysis) improves the ill-conditioned nature of the problem. Both these contributions lead to a more stable and convergent inversion process.

Small errors in our V_s estimates or in the selection of a realistic V_p/V_s ratio are acceptable because the V_p model derived from them is used as an approximate reference rather than as exact hard model data.

If there are severe errors in the surface-wave V_s estimates (for example, higher-mode energy mistakenly selected for fundamental mode during the dispersion-curve analysis phase of MASW (Park et al., 1999b), or if the basic assumption about the V_p/V_s ratio (e.g., that the general trend of V_p follows the general trend of V_s) is not reasonably close to true, then the estimated pseudo V_p model may fall outside the minimizing (objective) function valley of the true solution. In such instances, the JARS solution may be different signifi-

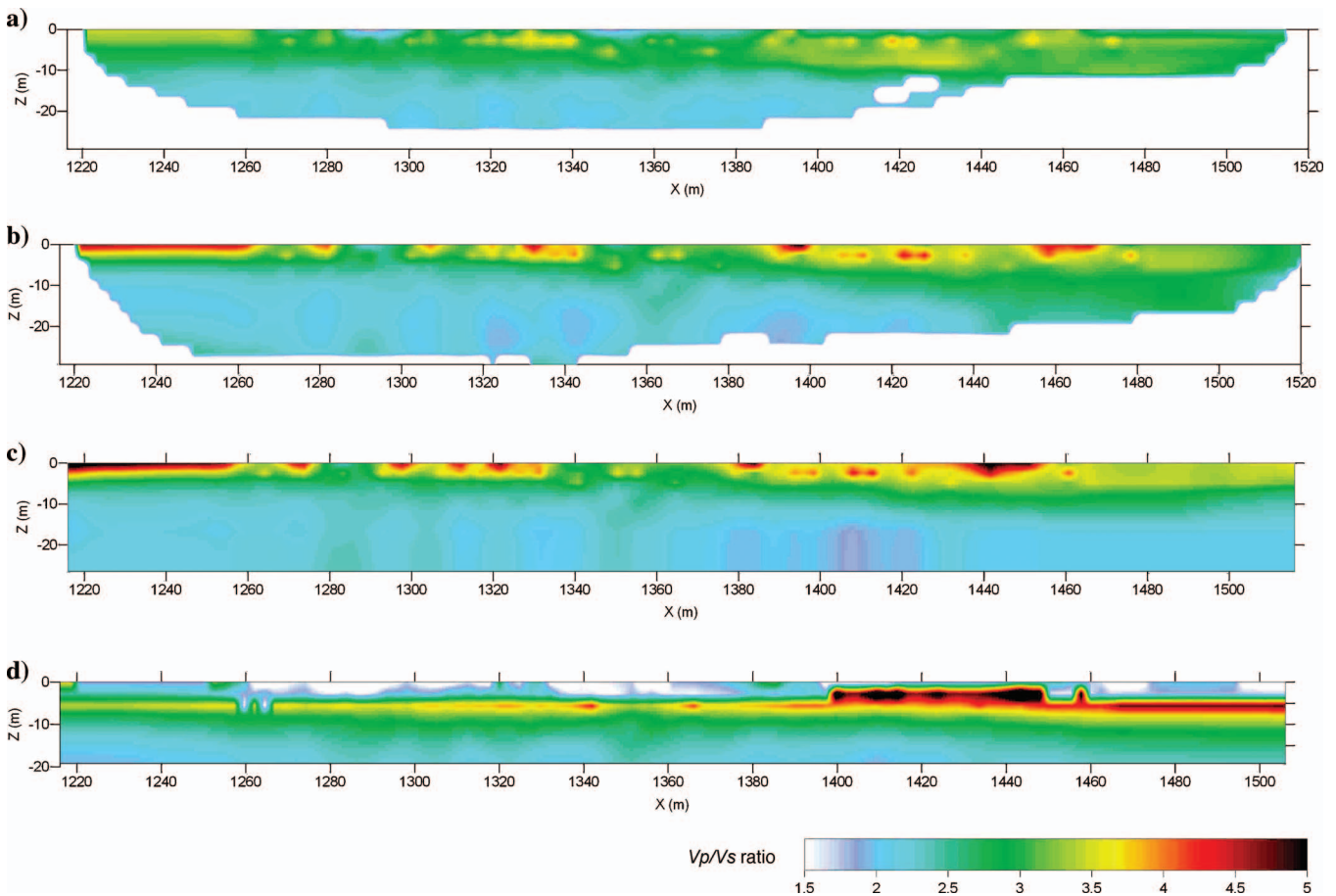


Figure 6. V_p/V_s ratio maps using the inverse refraction travelt ime problem and MASW solutions for the seismic data set collected in the Sonora Desert, Arizona, USA. (a) JARS method V_p/V_s ; (b) Tomography only with second-order smoothing constraints V_p/V_s ; (c) Tomography only with first-order smoothing constraints V_p/V_s ; and (d) GRM two-layer solution V_p/V_s (Kriging was applied to the solution data to create the image).

cantly from the true solution. However, in both cases, other geologic and geophysical observations and data will provide important clues as to the accuracy of the V_s estimate and V_p/V_s ratio, thereby minimizing the risk of erroneous interpretation of V_p maps.

Analyses of example data illustrate how current refraction/tomography algorithms (without using additional API) arbitrarily pick a solution among an uncontrolled range of possible solutions (similar to the example in Figure 2). The specific solution selected depends more on the algorithm's intrinsic properties, such as model preferences, smoothing constraints (order and weight), maximum allowable values, and preferred spatial gradients of the results rather than site specific knowledge. For example, the delay-time method (GRM and other refraction methods) would pick a two-layer solution (model preference) because there are two apparent slopes interpretable in the first arrivals and would thus force a two-layer model solution. This solution would be positioned at one end of the nonuniqueness valley, toward the maximum vertical-gradient region (the triangle on Figure 2). The influence of the smoothing constraints — in the vertical direction, tomography-only algorithms — would force a solution toward the minimum vertical-gradient region in the nonuniqueness valley (the filled circles on Figure 2). The order and weight of the smoothing constraints would influence the exact location. Inversion behavior of this kind has been observed for modeled synthetic data when using conventional delay-time analysis (refraction) and three commercial refraction-tomography codes (Sheehan and Doll, 2003).

So far we have assumed that the infinite earth continuum is adequately represented by a finite number of model parameters and that the data (measured first arrivals) are exact. However, in reality, all these assumptions are violated. The presence of data and model errors (as well as other types of errors) will increase the distance between the concrete (that is, the estimated solution \mathbf{s}^{est}) and the abstract (that is, the absolute true solution \mathbf{s}^{true}) (Figure 3).

The JARS method could also be applied to solving the shear-wave IRTP. Such an approach would be appropriate for calculating high-resolution V_s maps beyond what can be achieved using the MASW method. Surface-wave propagation and associated particle motions tend to smear special sampling as a function of depth (wavelength). This smearing phenomenon decreases V_s lateral resolution with depth and therefore smoothes the final 2D V_s model. Because the JARS method incorporates the MASW V_s model as the reference, it has the potential to produce a more detailed V_s IRTP solution in comparison with MASW results because it does not suffer from the long wave-length smearing.

CONCLUSIONS

We propose using surface-wave information to constrain the inverse refraction-traveltime problem. The V_s estimated from surface-wave analysis is included in the general inversion, and it helps reduce the nonuniqueness of the possible solutions. Experimental results from the application of the joint analysis of refractions with the surface-waves method demonstrate that the new algorithm enhances the analysis of first arrivals for velocity field estimation and yields a more plausible and geologically realistic solution by including additional data. The joint analysis of refractions with the surface waves method requires that both V_p and V_p/V_s ratio maps appear realistic in order to accept the final solution, whereas existing inverse-refraction-traveltime-problem algorithms most often provide unrealistic V_p/V_s ratio estimates.

Future directions for research may include the use of expert systems for better approximation of V_p/V_s ratio trends at specific sites or the use of first arrival amplitudes to help resolve the inverse refraction-traveltime-problem nonuniqueness.

ACKNOWLEDGMENTS

The authors would like to thank Ross Black, Doug Walker, and Chris Allen for their useful comments and suggestions and Mary Brohammer and Marla Adkins-Heljeson for assistance in manuscript preparation and submission. We appreciate the comments and suggestions of Yonghe Sun, William Harlan, Paul Docherty, Samuel Gray, and an anonymous reviewer, which have improved the final form of the manuscript.

REFERENCES

- Ackerman, H. D., L. W. Pankratz, and D. Dansereau, 1986, Resolution of ambiguities of seismic refraction traveltime curves: *Geophysics*, **51**, 223–235.
- Backus, G. E., and J. F. Gilbert, 1967, Numerical applications of a formalism for geophysical inverse problem: *Geophysical Journal of the Royal Astronomical Society*, **13**, 247–276.
- 1968, Resolving power of gross earth data: *Geophysical Journal of the Royal Astronomical Society*, **16**, 196–205.
- 1970, Uniqueness in the inversion of inaccurate gross earth data: *Philosophical Transactions of the Royal Society of London, Ser. A*, **266**, 123–192.
- Burger, H. R., 1992, *Exploration geophysics of the shallow subsurface*: Prentice Hall, Inc.
- Claerbout, J. F., 1992, *Earth sounding analysis: Processing versus inversion*: Blackwell Science Publications.
- Constable, S. C., R. L. Parker, and C. G. Constable, 1987, Occam's inversion: A practical algorithm for generating smooth models from electromagnetic sounding data: *Geophysics*, **52**, 289–300.
- Delprat-Jannaud, F., and P. Lailly, 1993, Ill-posed and well-posed formulations of the reflection travel time tomography problem: *Journal of Geophysical Research*, **98**, 6589–6605.
- Hansen, C., 1998, Rank-deficient and discrete ill-posed problems, Numerical aspects of linear inversion: *Society of Industrial and Applied Mathematics*.
- Healy, J. H., 1963, Crustal structure along the coast of California from seismic-refraction measurements: *Journal of Geophysical Research*, **68**, 5777–5787.
- Ivanov, J., R. D. Miller, J. Xia, D. Steeples, and C. B. Park, 2005a, The inverse problem of refraction traveltimes, Part I: Types of geophysical nonuniqueness trough minimization: *Pure and Applied Geophysics*, **162**, 447–459.
- , 2005b, The inverse problem of refraction traveltimes, Part II: Quantifying refraction nonuniqueness using a three-layer model: *Pure and Applied Geophysics*, **162**, 461–477.
- Ivanov, J., C. B. Park, R. D. Miller, and J. Xia, 2000a, Mapping Poisson's Ratio of unconsolidated materials from a joint analysis of surface-wave and refraction events: *Proceedings of the 13th Symposium on the Application of Geophysics to Engineering and Environmental Problems, EEGS*, 11–20.
- 2000b, Joint analysis of surface-wave and refracted events from river-bottom sediments: 70th Annual International Meeting, SEG, Expanded Abstracts, 1307–1310.
- Jaynes, E. T., 2003, *Probability theory: The logic of science*: Cambridge University Press.
- Last, B. J., and K. Kubik, 1983, Compact gravity inversion: *Geophysics*, **48**, 713–721.
- Lay, T., and T. Wallace, 1995, *Modern global seismology*: Academic Press Inc.
- Meju, M. A., 1994, Biased estimation: A simple framework for inversion and uncertainty analysis with prior information: *Geophysical Journal International*, **119**, 521–528.
- Menke, W., 1989, *Geophysical data analysis: Discrete inverse theory*: Academic Press Inc.
- Miller, R. D., J. Xia, C. B. Park, and J. Ivanov, 1999a, Multichannel analysis of surface waves to map bedrock: *The Leading Edge*, **18**, 1392–1396.
- Miller, R., J. Xia, C. B. Park, J. Davis, W. Shefchik, and L. Moore, 1999b, Seismic techniques to delineate dissolution features in the upper 1000 ft at a power plant: 69th Annual International Meeting, SEG, Expanded Ab-

- stracts, 492–495.
- Nolet, Guust, 1987, Seismic wave propagation and seismic tomography, in G. Nolet, ed., *Seismic tomography*: D Reidel Publishing Company.
- Palmer, D., 1980, The generalized reciprocal method of seismic refraction interpretation: SEG.
- Park, C. B., J. Ivanov, R. D. Miller, J. Xia, and N. Ryden, 2001, Multichannel analysis of surface waves (MASW) for pavement: Feasibility test: Proceedings of the 5th International Symposium, Society of Exploration Geophysicists of Japan, 25–30.
- Park, C. B., R. D. Miller, and J. Xia, 1999a, Multichannel analysis of surface waves: *Geophysics*, **64**, 800–808.
- Park, C. B., R. D. Miller, J. Xia, J. A. Hunter, and J. B. Harris, 1999b, Higher mode observation by the MASW method: Proceedings of the 69th Annual International Meeting, SEG, Expanded Abstracts, 524–527.
- Park, C. B., R. D. Miller, J. Xia, and J. Ivanov, 2000, Multichannel analysis of underwater surface wave near B. C. Vancouver, Canada: Proceedings of the 70th Annual International Meeting, SEG, Expanded Abstracts, 1303–1306.
- Portniaguine, O., and M. S. Zhdanov, 1999, Focusing geophysical inversion images: *Geophysics*, **64**, 874–887.
- Rudin, L. I., S. Osher, and E. Fatemi, 1992, Nonlinear total variation based noise removal algorithms: *Physica D: Nonlinear Phenomena*, **60**, 259–268.
- Ryden, N., C. B. Park, R. D. Miller, J. Xia, and J. Ivanov, 2001, High frequency MASW for non-destructive testing of pavements: Proceedings of the 14th Symposium on the Application of Geophysics to Engineering and Environmental Problems, EEGS, RBA-5.
- Sheehan, J., and W. Doll, 2003, Evaluation of refraction tomography codes for near-surface applications: Proceedings of the 73rd Annual International Meeting, SEG, Expanded Abstracts, 1235–1238.
- Slichter, L. B., 1932, The theory of interpretation of seismic traveltime curves in horizontal structures: *Physics*, **3**, 273–295.
- Tikhonov, A. N., and V. Y. Arsenin, 1977, *Solutions of ill-posed problems*: John Wiley and Sons.
- Xia, J., C. Chen, G. Tian, R. D. Miller, and J. Ivanov, 2005, Resolution of high-frequency Rayleigh-wave data: *Journal of Environmental and Engineering Geophysics*, **10**, 99–110.
- Xia, J., R. D. Miller, C. B. Park, J. A. Hunter, and J. B. Harris, 2000, Comparing shear-wave velocity profiles from MASW with borehole measurements in unconsolidated sediments, Fraser River B. C. Delta, Canada: *Journal of Environmental and Engineering Geophysics*, **5**, 1–13.
- Xia, J., R. D. Miller, and C. B. Park, 1999a, Estimation of near-surface shear-wave velocity by inversion of Rayleigh wave: *Geophysics*, **64**, 691–700.
- Xia, J., R. D. Miller, C. B. Park, J. A. Hunter, and J. B. Harris, 1999b, Evaluation of the MASW technique in unconsolidated sediments: Proceedings of the 69th Annual International Meeting, SEG, Expanded Abstracts, 437–440.
- Zhang, J., and M. N. Toksoz, 1998, Nonlinear refraction traveltime tomography: *Geophysics*, **63**, 1726–1737.
- Zhdanov, M. S., 2002, *Geophysical inverse theory and regularization problems*: Elsevier Science Publishing Company, Inc.